ANL-87-47
Distribution Category:
Energy Conservation--
Industry (UC-95f)

ANL--87-47

DE88 010068

Argonne National Laboratory
9700 South Cass Avenue
Argonne, Illinois 60439

SOME ISSUES CONCERNING FLUIDELASTIC INSTABILITY OF A GROUP OF CIRCULAR CYLINDERS IN CROSSFLOW

by

S. S. Chen

Materials and Components Technology Division

April 1988

DISCLAIMER

LEGIBILITY NOTICE

A major purpose of the Technical Information Center is to provide the broadest dissemination possible of information contained in DOE's Research and Development Reports to business, industry, the academic community, and federal, state and local governments.

Although a small portion of this report is not reproducible, it is being made available to expedite the availability of information on the research discussed herein.

1

CONTENTS

FIGURES

TABLES

NOMENCLATURE

Symbol	Description
C_s	Viscous damping coefficient of a structure
D	Diameter of a cylinder (= 2R)
EI	Flexural rigidity of a cylinder
f	Oscillation frequency
f_v	Natural frequency in vacuum
g_j	Fluid force component in the x direction of the jth cylinder
h_j	Fluid force component in the y direction of the jth cylinder
ℓ	Cylinder length
m	Cylinder mass per unit length
N	Number of cylinders in an array
P	Pitch
R	Radius of a cylinder (= D/2)
Re	Reynolds number
t	Time
T	Transverse pitch
u_j	Displacement of the jth cylinder in the x direction
U	Gap flow velocity in a tube array
U_v	Reduced flow velocity (= U/f_vD)
v_j	Displacement of the jth cylinder in the y direction
x,y,z,	Cartesian coordinates
$\alpha_{jk},\beta_{jk},\sigma_{jk},\tau_{jk}$	Added-mass coefficients
$\alpha'_{jk},\beta'_{jk},\sigma'_{jk},\tau'_{jk}$	Fluid damping coefficients
$\alpha'_{ojk},\beta'_{ojk},\sigma'_{ojk},\tau'_{ojk}$	Fluid viscous damping coefficients at zero flow velocity
$\alpha''_{jk},\beta''_{jk},\sigma''_{jk},\tau''_{jk}$	Fluid stiffness coefficients
$\bar{\alpha}'_{ojk},\bar{\beta}'_{ojk},\bar{\sigma}'_{ojk},\bar{\tau}'_{ojk}$	Fluid viscous damping at zero flow velocity
γ	$= \rho\pi R^2/m$
γ_{pq}	Added mass matrix
ζ	Damping ratio
ζ_v	Damping ratio in vacuum
μ_p	Eigenvalue of added-mass matrix, γ_{pq}

ρ	Fluid density
ω_v	Natural frequency in radian in vacuum

Subscripts

j,k	Cylinder number j,k (j,k = 1 to N)
p,q	1 to 2N
v	Parameters measured in vacuum

SOME ISSUES CONCERNING FLUIDELASTIC INSTABILITY OF A GROUP OF CIRCULAR CYLINDERS IN CROSSFLOW

S. S. Chen

ABSTRACT

Since the early 1970s, extensive studies of fluidelastic instability of circular cylinders in crossflow have been reported. A significant understanding of the phenomena involved now exists. However, some confusion, misunderstanding, and misinterpretation still remain. The objective of this report is to discuss, on the basis of the current state of the art, a series of the most asked questions. Emphasis is placed on the determination of the critical flow velocity, nondimensional parameters, stability criteria, and instability mechanisms.

I. INTRODUCTION

A group of circular cylinders submerged in crossflow can be subjected to dynamic instability, typically referred to as fluidelastic instability. The threshold flow velocity at which cylinders undergo large oscillations is called the critical flow velocity. If a system component is operated at a flow velocity above the critical value, severe damage to the component is likely to occur, often after a short time of operation. Therefore, operation at a flow velocity above the critical value is generally not acceptable.

Since the early 1970s, extensive studies of fluidelastic instability have been reported. The studies include empirical stability criteria, mathematical models, scale-model and full-scale evaluation tests, and design assessment. A significant understanding of the problem now exists. However, some confusion, misunderstanding, and misinterpretation still remain. As a matter of fact, fluidelastic instability is probably one of the most debated and confusing topics in the area of fluid-structure interactions. For example, erroneous descriptions of the instability mechanism have been published in journals, these erroneous descriptions have been quoted by others working in this subject area, and the same physical phenomena have been given different interpretations.

At present, it is still not possible to predict the instability phenomena from fundamental principles of fluid dynamics and the theory of elasticity, and some of the physics associated with the instability are not well understood. However, with available information, some of the unnecessary misunderstanding and confusion can be avoided. The objective of this report is to discuss several important issues on the basis of the unsteady flow model.

There are hundreds of publications on this subject. A literature survey will not be given in this report since several surveys have recently appeared in the literature [e.g., Paidoussis 1987, Weaver and Fitzpatrick 1987]. It should be noted that significant contributions have been made by investigators in different countries, and progress is being made on different aspects of the problem.

II. HOW SHOULD ONE DETERMINE THE CRITICAL FLOW VELOCITY?

The critical flow velocity is defined as the flow velocity above which cylinders undergo large oscillations. Mathematically, this is generally described as follows: Let the displacement of a particular cylinder be

$$u_j(t) = a_j \exp(\lambda + i\omega t)t \ . \tag{1}$$

The stability of the cylinder is determined by λ, which is a function of flow velocity U. If $\lambda < 0$, the cylinder motion is damped; if $\lambda > 0$, the cylinder displacement increases with time until nonlinear effects become important. Therefore, the critical flow velocity can be determined from the condition $\lambda = 0$.

The value of λ is related to the modal damping ratio ζ_f in flow. For cylinders oscillating in a specific mode (see Appendix),

$$\lambda = -\zeta_f \omega_f \ , \tag{2}$$

where ω_f is the oscillation frequency in flow. When the modal damping ratio ζ_f is smaller than zero, the cylinders lose stability. Therefore, the flow velocity at which a modal damping ratio becomes zero is the critical flow velocity. Although this is the most precise method to determine the critical flow velocity, in practice, it has not been used because it takes much more time to measure the modal damping ratio as a function of flow velocity. A number of other methods that have been used to define the critical flow velocity in laboratory and practical equipment tests are presented below.

Velocity Amplitude vs. Flow Velocity

The response (acceleration, velocity, displacement, or strain) amplitude is plotted as a function of flow velocity. This may be plotted in linear or logarithmic scale, as shown in Fig. 1. The critical flow is determined from the curve and defined as the flow velocity at which the cylinder experiences a rapid increase in response. Cylinder response curves depend on cylinder damping. Figure 1 shows typical response curves for small and large damping. For small damping, turbulence excitation contributes to significant cylinder oscillations and the critical flow velocity is more difficult to determine because of the interaction between turbulence buffeting and fluidelastic instability. On the other hand, for high values of damping at

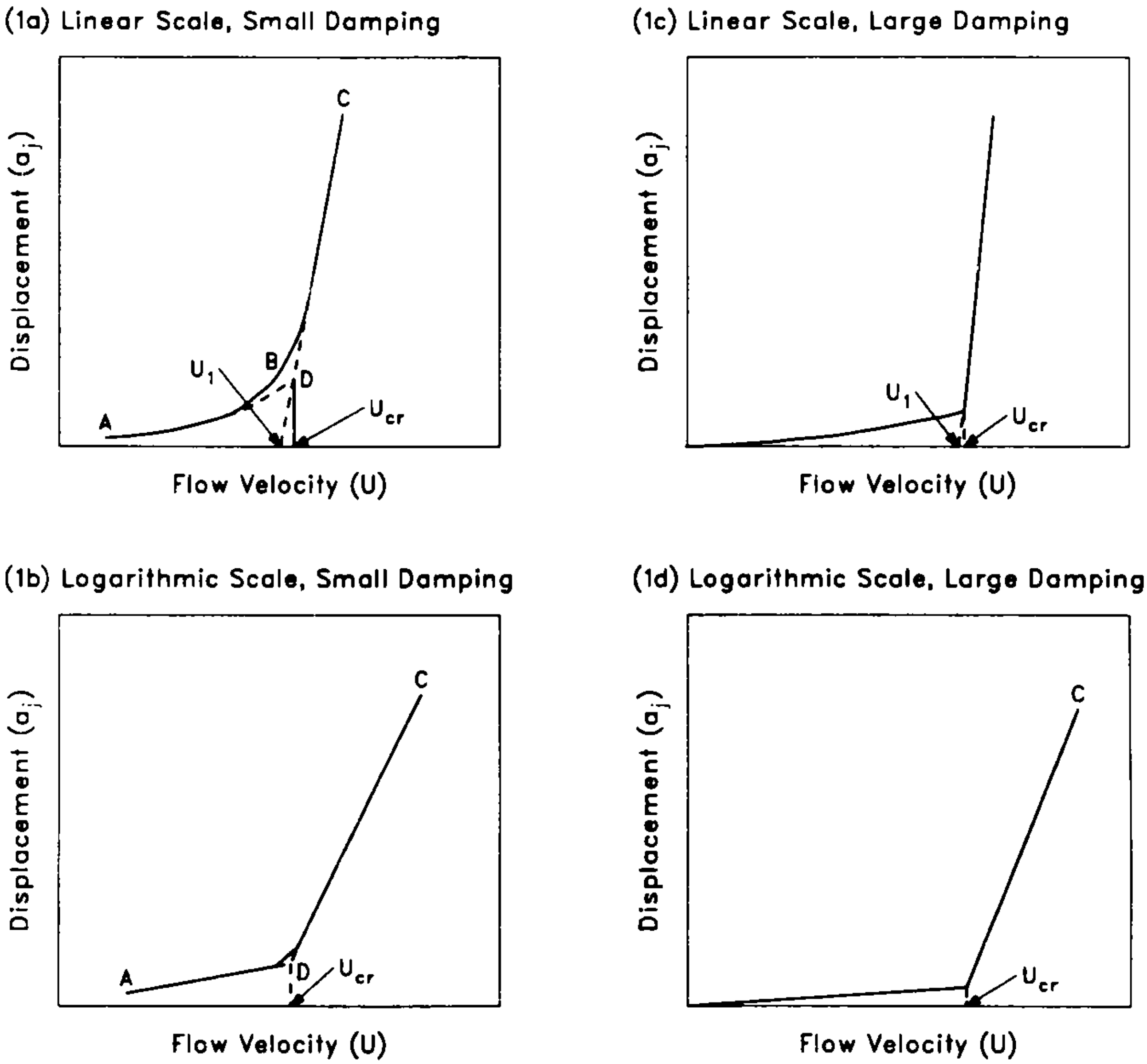

Fig. 1. Vibration amplitude vs. flow velocity

the critical flow velocity, cylinder response increases very rapidly with a small increase in flow and, in general, it is not difficult to define the critical flow velocity.

In practice, no consistent methods have been used to define the critical flow velocity. For example, on a linear scale, Weaver and El-Kashlan (1981) define the critical flow velocity as the point on the curve where there is a sudden change in slope. This definition is acceptable if the change is very sudden. It would be difficult to determine the critical flow velocity when the change is more gradual as that given in Fig. 1a. Soper (1980) defines the critical flow velocity as the point at which a tangent to the postcritical response intersects the velocity axis; this is given by U_1 in Figs. 1a and 1c. In general, this method underestimates the critical flow velocity.

In the subcritical flow velocity range, the cylinder displacement is proportional to U^b, where b varies from about 1 to 2. A more precise definition of the critical flow velocity is the U_{cr} given in Figs. 1a and 1b, which is defined as the intersection point of the tangent to the postcritical response curve and a curve proportional to U^b passing point A. The difficulty of this method is that the value of b is generally not known. An alternate method is to extend the subcritical response curve smoothly to intersect the tangent of the postcritical response curve at point D in Figs. 1a and 1c.

On a logarithmic scale, the critical flow velocity is easier to define. In general, both response curves in the subcritical region and postcritical region are basically straight lines. The slope in the subcritical region varies from 1 to 2 whereas in the postcritical region it can vary from 5 to 20. The intersection of these two lines gives the critical flow velocity. Although this method is better, it has not been used frequently (Axisa et al. 1984, Price and Paidoussis 1987).

Frequency Spectra as a Function of Flow Velocity

A group of cylinders subjected to crossflow exhibits broad-band response in the subcritical flow regime. In the postcritical regime, a particular mode is dominant and the frequency spectra contain a narrow-band peak (see Fig. 2). Therefore, the critical flow velocity is defined as the flow velocity at which the response power spectral density (PSD) changes from a relatively broad-band spectrum to a narrow-band spectrum (Chen and Jendrzejczyk 1986). For a heavy fluid, this method is appropriate. However, in a light fluid, the natural frequencies of coupled modes occur in a narrow band. There is very little difference in the spectra before and after instability occurs.

Amplitude Distribution as a Function of Flow Velocity

Amplitude distribution as a function of flow velocity is a plot which displays probability density vs. normalized amplitude. The probability is determined by the ratio of the time that the cylinder response is within an

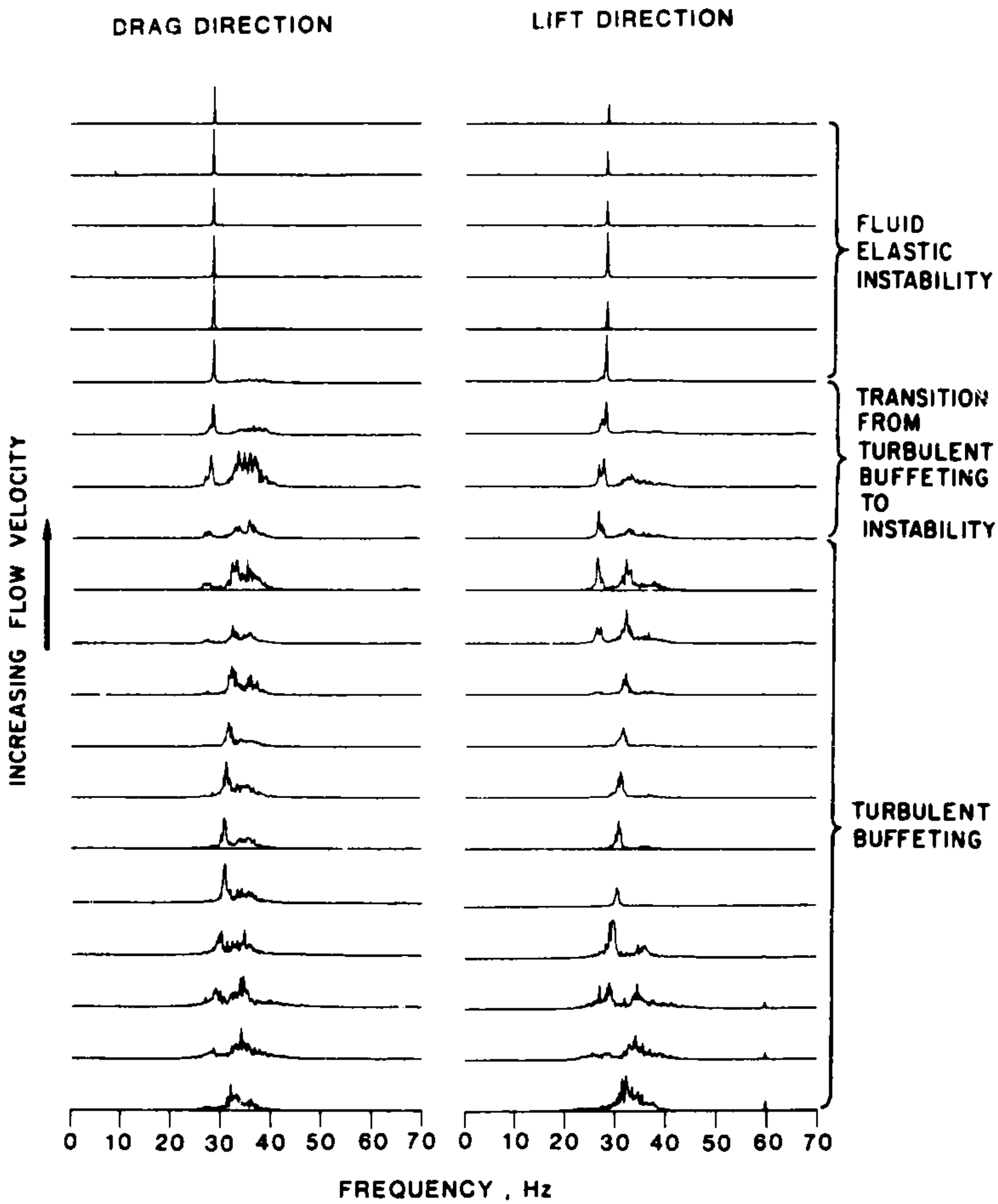

Fig. 2. Cylinder response PSDs for various flowrates

amplitude window to the total time the response is sampled. A random signal will produce the Gaussian bell-shaped probability density function and a periodic or discrete signal will produce a saddle-shaped probability density function. For example, Fig. 3 shows the amplitude distribution at the subcritical and postcritical regions. It is fairly easy to distinguish the periodic component from narrow- and wide-band response. This technique has not been utilized in practice.

Coherence and Phase Functions of Cylinder Response

In fluidelastic instability regimes, motion of adjacent cylinders is highly correlated with the coherence function of the response of adjacent cylinders close to 1.0 and the phase function is almost constant over a large frequency range. In subcritical regimes, the coherence function is typically less than 0.5 and the phase function is randomly distributed over the whole frequency range. In other words, as the flow velocity increases from the subcritical regime to the postcritical regime, the cylinder motion is drastically changed from a random vibration to an almost periodic, deterministic motion. Therefore, the critical flow velocity can be determined on the basis of the drastic changes of the coherence and phase functions. Axisa et al. (1986) attempted to determine critical flow velocities by using coherence functions. Their results were consistent with those based on the plots of amplitude vs. flow velocity.

Other Methods

Several other methods can also be used to identify the critical flow velocity.

- Sensory Observations: Structural response amplitudes are determined visually or auditorily. This method requires engineering judgment and experience and, in general, does not provide accurate determination of U_{cr}.

- Threshold Response Amplitude vs. Flow Velocity: The critical flow velocity is defined as the flow velocity at which the response amplitude exceeds a certain limit. For example, Yeung and Weaver (1983), and Minakami and Ohtomi (1987) define the permissible limit as 2.5% of cylinder diameter. This method is straightforward and practically convenient, but theoretically not correct.

- Time History: Structural responses in subcritical flow regimes and postcritical regimes are different. Time history can be used to determine the state of the system (see Fig. 3). In some cases, spatial plots of structural responses are particularly useful in determining the critical flow velocity.

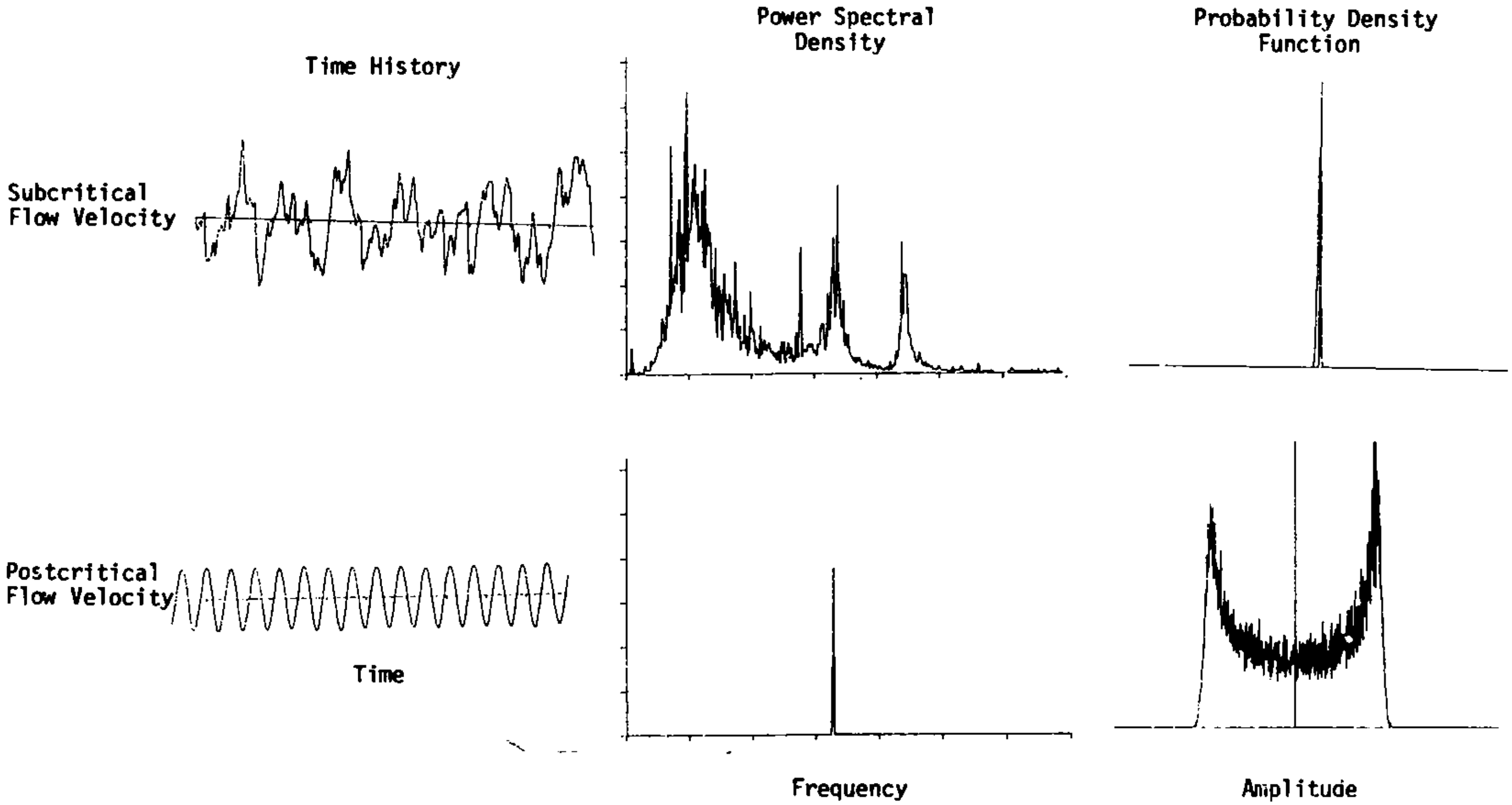

Fig. 3. Time histcries, power spectra, and probability density functions of cylinder response

Depending on the circumstances, different methods can be used in practical cases. In most cases, the vibration amplitude vs. flow velocity is most useful. Frequently, it is sufficient to determine the critical flow velocity. If difficulty is encountered, the amplitude distribution as a function of flow velocity can be used for light fluid whereas the frequency spectra as a function of flow velocity can be used for heavy fluid. Of course, the method that uses the modal damping ratio ζ_f is the most precise, but the measurement of ζ_f may be difficult.

Several complications hamper the determination of the critical flow velocity.

- Vortex-Induced Oscillations: For heavy fluids, vortex-induced lock-in oscillations and fluidelastic instability may occur in the same range of flow velocity. One or more peaks appear in response curves in some cases. Under these circumstances, precise determination becomes more difficult, in particular, when lock-in oscillations and fluidelastic instability occur at the same flow velocity. Some of these examples have been reported by Weaver and El-Kashlan (1981).

- Hysteresis: In heavy fluids, two critical flow velocities are present, i.e., intrinsic critical flow velocity and excited critical flow velocity (Chen and Jendrzejczyk 1987, Hara 1987). The difference between the two limits can be as much as 30% (see Fig. 4). In most cases, the intrinsic critical flow velocity is reported. However, some of the reported data may be associated with the excited critical flow velocity. Theoretically, the stability limit from the linear theory is the intrinsic instability. Practically, if the system is subjected to transient overflow, the excited critical flow velocity must be considered.

From the above considerations, it is clear that the critical flow velocity is simple to define, but, in practice, it may be difficult to determine. The same set of data given to two different researchers may result in two different critical flow velocities.

III. WHAT PARAMETERS SHOULD BE USED?

The three important parameters used in the stability criteria are mass per unit length m, natural frequency f, and damping ratio ζ. For a group of cylinders vibrating in flow, the definition of these three parameters varies widely. These parameters can be defined under at least the following four different conditions:

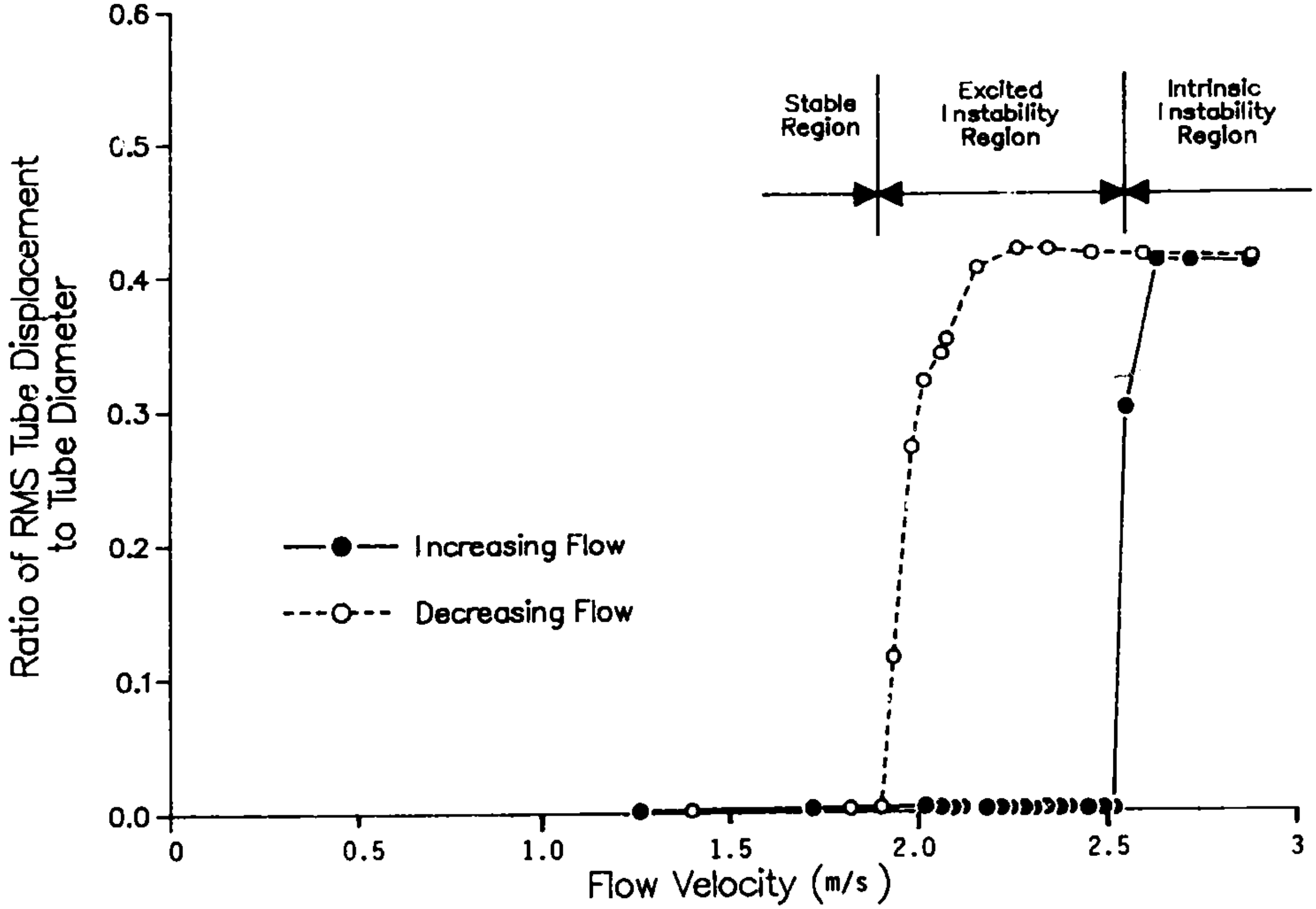

Fig. 4. Tube displacement as a function of flow velocity

(1) In Vacuum (m_v, f_v, ζ_v): System parameters are measured in vacuum (practically, in air); the effect of the surrounding fluid is ignored (all fluid force coefficients are equal to zero).

(2) In Quiescent Fluid - Uncoupled Vibration (m_u, f_u, ζ_u): System parameters are measured for an elastic cylinder vibrating in a fluid with the surrounding cylinders being rigid (all fluid-force coefficients are equal to zero except α_{jj}, α'_{jj}, or β_{jj} and β'_{jj}).

(3) In Quiescent Fluid - Coupled Vibration (m_c, f_c, ζ_c): System parameters are measured for an array of cylinders vibrating in fluid; the coupling among different cylinders that is due to fluid is included (including fluid inertia and fluid viscous damping).

(4) In Flow (m_f, f_f, ζ_f): System parameters are measured in flow for uncoupled and/or coupled modes; in general, they are dependent on the flow velocity.

These parameters, under different conditions, are summarized in Table 1. It should be noted that, in a group consisting of N identical cylinders, m, f, and ζ are not a single set of numbers except in vacuum. In quiescent fluid, for coupled or uncoupled vibration, there are 2N natural frequencies and modal damping values, which are not necessarily the same. In flow, there are 2N coupled modes which are functions of flow velocity. Therefore, f_f and ζ_f are functions of flow velocity.

Questions have been raised regarding which set of parameters should be used. In the literature, many variations have been utilized in reporting the

Table 1. Effective mass, natural frequency, and modal damping ratio under different conditions

Parameters	In vacuum	In quiescent fluid: Uncoupled vibration	In quiescent fluid: Coupled vibration	In flow: Uncoupled and/or coupled modes
Effective mass	m_v	m_u	m_c	m_f
Natural frequency	f_v	f_u	f_c	f_f
Modal damping ratio	ζ_v	ζ_u	ζ_c	ζ_f

data; these include (1) m_v, f_v, ζ_v; (2) m_u, f_u, ζ_u; (3) m_f, f_f, ζ_f; (4) m_v, f_v, ζ_f; (5) m_u, f_f, ζ_u, etc. It is apparent that all these sets cannot be correct theoretically and the correlations developed from the data can be expected to be dependent on the parameter set chosen.

From theoretical and practical considerations, the set of parameters determined in vacuum, m_v, f_v, and ζ_v, is the most convenient to use. It is well defined and there is only one set of numbers. However, when there exists additional damping associated with fluid effects, other than the viscous fluid damping associated with $\bar{\alpha}'_{ojk}$, $\bar{\sigma}'_{ojk}$, $\bar{\tau}'_{ojk}$, and $\bar{\beta}'_{ojk}$ (see Appendix), such as fluid damping in the gap of the tube/baffle clearance of heat exchanger tubes, these damping effects should be properly accounted for.

Other sets of parameters can also be used. For example, m_u, f_u, ζ_u can be conveniently used for a flexible cylinder in a rigid array. If a set of parameters is to be applied to an array of flexible cylinders, a decision must be made on the proper set of m_u, f_u, and ζ_u, since there are 2N sets which may be distinct. In this case, the set corresponding to the instability mode should be used. Some investigators use the in-flow values, m_f, f_f, ζ_f. Since these in-flow values depend on flow velocity, it is difficult to use these parameters. Furthermore, some investigators use m, f, and ζ for mixed conditions, such as m_u, f_v, and ζ_v. This practice is not convenient and may be theoretically incorrect.

The parameters in the stability criterion can be determined on the basis of the unsteady flow model. The stability criterion may be expressed in terms of different sets of parameters. However, the stability criteria obtained using different sets of parameters are different. In the literature, some of the criteria are established without proper justification. This is another reason for the scattering of data on stability diagrams. In evaluating reported data, it is important to be aware of the parameters used by particular investigators.

On the basis of the equations of motion for cylinders, Navier-Stokes equations, and appropriate boundary conditions, it is straightforward to show that the critical reduced flow velocity depends on the nondimensional parameters ζ, Re, m_r, U_v, u_j^*, and v_j^* (Chen 1986), where

$$\begin{aligned} \zeta &= \frac{C_s}{2m\omega_v}, \qquad & U_v &= \frac{U}{f_v D}, \\ Re &= \frac{\rho D U}{\mu}, \qquad & u_j^* &= \frac{u_j \omega_v}{U}, \\ m_r &= \frac{m}{\rho D^2}, \qquad & v_j^* &= \frac{v_j \omega_v}{U}, \end{aligned} \tag{3}$$

and μ is fluid viscosity (see Appendix). Therefore,

$$U_r = F(\zeta, m_r, Re, u_j^*, v_j^*) \ . \tag{4}$$

The critical reduced flow velocity depends on the nondimensional, subcritical oscillation amplitudes u_j^* and v_j^*. When u_j^* and v_j^* are very small, the critical flow velocity is the intrinsic instability flow velocity. When the effects of u_j^* and v_j^* cannot be ignored, the critical flow velocity will most likely be the excited instability flow velocity.

In most practical applications, the effect of subcritical oscillations on the critical flow velocity can be neglected and Eq. (4) may be written as

$$U_r = F(\zeta, m_r, Re) \ . \tag{5}$$

Experimental data show that the critical flow velocity does not vary significantly with Re; therefore,

$$U_r = F(\zeta, m_r) \ , \tag{6}$$

where ζ and m_r are the two separate parameters which characterize the stability criteria.

IV. WHAT ARE THE INSTABILITY MECHANISMS?

Theoretically, instability occurs when

$$\zeta_f = 0 \ . \tag{7}$$

For flow velocities larger than the critical flow velocity, ζ_f will be a negative value and the system motion will be amplified. This can be seen from the equation of motion of cylinders in crossflow [see Eqs. (A.7) and (A.8) in the Appendix]

$$[M]\{\ddot{Q}\} + [C]\{\dot{Q}\} + [K]\{Q\} = \{G\} \ , \tag{8}$$

where $[M]$ is the mass matrix, $[C]$ is the damping matrix, $[K]$ is the stiffness matrix, $\{Q\}$ is the generalized structural displacement vector, and $\{G\}$ is the excitation force vector. By premultiplying $\{\dot{Q}\}^T$ and forming the symmetric and antisymmetric components of the resulting matrices,

$$[M_1] = \frac{1}{2}\left([M] + [M]^T\right) , \quad [M_2] = \frac{1}{2}\left([M] - [M]^T\right) ,$$

$$[C_1] = \frac{1}{2}\left([C] + [C]^T\right) , \quad [C_2] = \frac{1}{2}\left([C] - [C]^T\right) , \tag{9}$$

and

$$[K_1] = \frac{1}{2}\left([K] + [K]^T\right) , \quad [K_2] = \frac{1}{2}\left([K] - [K]^T\right) ,$$

we can separate terms and obtain the following:

$$\{\dot{Q}\}^T[M_1]\{\ddot{Q}\} + \{\dot{Q}\}^T[C_2]\{\dot{Q}\} + \{\dot{Q}\}^T[K_1]\{Q\}$$
$$= -\left(\{\dot{Q}\}^T[M_2]\{\ddot{Q}\} + \{\dot{Q}\}^T[C_1]\{\dot{Q}\} + \{\dot{Q}\}^T[K_2]\{Q\}\right) + \{\dot{Q}\}^T\{G\} . \tag{10}$$

Equation (10) equates rates of work. The terms on the right side produce a net work resultant, the magnitude of which, when integrated over a closed path through the space $\{Q\}$, depends on the path taken. The forces corresponding to the matrices $[M_2]$, $[C_1]$, and $[K_2]$, appearing on the right side, are thus, by definition, the nonconservative parts of the forces represented by $[M]$, $[C]$, and $[K]$. Similarly, the terms on the left side can be shown to give rise to a zero work resultant over any closed path, and therefore, together are the sum of the rates of work from the potential forces and the rate of change of kinetic energy.

Different types of instability mechanisms can be determined from Eq. (10):

- Fluid-damping-controlled Instability (Single Mode Flutter): The dominant terms are associated with the symmetric damping matrix $[C_1]$. Flutter arises because the fluid dynamic forces create "negative damping," that is, a fluid force that acts in phase with the structural velocity.

- Fluid-stiffness-controlled Instability (Coupled-Mode Flutter): The dominant terms are associated with the antisymmetric stiffness matrix $[K_2]$. It is called coupled-mode flutter because a minimum of two modes are required to produce it.

All fluidelastic instabilities associated with Eq. (8) can be described by these two mechanisms. For an instability in which fluid damping is the controlling mechanism, we can consider a single degree of freedom. For example, the equation of motion in the x direction for a single elastic cylinder surrounded by a group of rigid cylinders is (see Appendix)

$$(1 + \gamma\alpha_{jj})\ddot{a}_j + \left(2\zeta_v\omega_v + \omega_v\alpha'_{ojj} - \frac{\gamma}{\pi^3} U_v^2 \frac{\omega_v^2}{\omega} \alpha'_{jj}\right)\dot{a}_j$$

$$+ \left(\omega_v^2 - \frac{\gamma}{\pi^3} U_v^2\omega_v^2\alpha''_{jj}\right)a_j = 0 \ . \tag{11}$$

The natural frequency ω_f, and modal damping ratio ζ_f in flow are

$$\omega_f = \left(\frac{1 - \frac{\gamma}{\pi^3} U_v^2\alpha''_{jj}}{1 + \gamma\alpha_{jj}}\right)^{0.5} \omega_v \ ,$$

$$\zeta_f = \frac{1}{1 + \gamma\alpha_{jj}} \left[\left(\zeta_v + \frac{1}{2}\alpha'_{ojj}\right) - \frac{\gamma}{2\pi^3} U_v^2\alpha'_{jj}\left(\frac{\omega_v}{\omega_f}\right)\right]\left(\frac{\omega_v}{\omega_f}\right) \ . \tag{12}$$

The critical flow velocity can be determined from $\zeta_f = 0$; i.e.,

$$U_v^2 = \frac{2\pi^3\left(\zeta_v + \frac{1}{2}\alpha'_{ojj}\right)}{\gamma\alpha'_{jj}} \left(\frac{\omega_f}{\omega_v}\right) \ . \tag{13}$$

This is the equation for fluid-damping-controlled instability, in which the instability is associated with the fluid damping, usually called negative damping. In this situation, where instability is controlled by fluid damping, the fluid damping force leads the cylinder displacement. The dominant fluid force coefficients are α'_{jj} and β'_{jj}. For an elastic cylinder in an array, the fluid damping coefficients α'_{jj} or β'_{jj} must be positive to make the cylinder unstable in the x or y direction.

For two elastic cylinders oscillating in the x direction, one of the coupled modes may become unstable. Which mode becomes unstable depends on the characteristics of the damping coefficients. For example, if both α_{jj} and $\alpha_{j,j+1}$ are positive, the instability will be associated with the two cylinders that are moving in phase. However, if α_{jj} is positive and $\alpha_{j,j+1}$ is negative, the two cylinders will oscillate out of phase.

For fluid-stiffness-controlled instability, the antisymmetric part of the stiffness matrix K_2 is the element that causes instability. Mathematically, it can be stated that the antisymmetric part of stiffness makes the effective damping less than zero.

Consider an example of two flexible cylinders, 1 and 2, oscillating in air flow. Cylinder 1 is moving only in the x direction while cylinder 2 is moving only in the y direction. Assume that the damping values of the cylinders are zero when the flow velocity is equal to zero. In this case the equations of motion are

$$\begin{aligned}
&\ddot{a}_1 - \frac{\gamma}{\pi^3} U_v^2\left(\frac{\omega_v^2}{\omega}\right)(\alpha'_{11}\dot{a}_1 + \sigma'_{12}\dot{b}_2) \\
&\quad + \omega_v^2 a_1 - \frac{\gamma}{\pi^3} U_v^2\omega_v^2(\alpha''_{11}a_1 + \sigma''_{12}b_2) = 0 , \\
&\ddot{b}_2 - \frac{\gamma}{\pi^3} U_v^2\left(\frac{\omega_v^2}{\omega}\right)(\tau'_{21}\dot{a}_1 + \beta'_{22}\dot{b}_2) \\
&\quad + \omega_v^2 b_2 - \frac{\gamma}{\pi^3} U_v^2\omega_v^2(\tau''_{21}a_1 + \beta''_{22}b_2) = 0 .
\end{aligned} \tag{14}$$

In order to illustrate the role of fluid stiffness on modal damping, we neglect the fluid damping associated with α'_{11}, σ'_{12}, τ'_{21}, and β'_{22}, as well as the diagonal terms of fluid stiffness coefficients α''_{11} and β''_{22}. Equations (14) become

$$\begin{aligned}
&\ddot{a}_1 + \omega_v^2 a_1 - \frac{\gamma}{\pi^3} U_v^2\omega_v^2\sigma''_{12}b_2 = 0 , \\
&\ddot{b}_2 + \omega_v^2 b_2 - \frac{\gamma}{\pi^3} U_v^2\omega_v^2\tau''_{21}a_1 = 0 .
\end{aligned} \tag{15}$$

Without the fluid stiffness coupling that is associated with σ''_{12} and τ''_{21}, the two cylinders are uncoupled with their natural frequency equal to ω_v and their modal damping equal to zero. With fluid stiffness coupling of σ''_{12} and τ''_{21}, it is straightforward to show that the natural frequency and modal damping ratio of Eqs. (15) are

$$\begin{aligned}
&\omega_f = \omega_v\sqrt{1 - \zeta_f^2} , \\
&\zeta_f = \pm \frac{\gamma}{2\pi^3} U_v^2\sqrt{\sigma''_{12}\tau''_{21}}\ \omega_v .
\end{aligned} \tag{16}$$

Therefore, the fluid stiffness terms associated with σ''_{12} and τ''_{21} reduce the natural frequency and contribute to damping. Note that the damping value is positive for one mode and negative for the other. If this damping plus the other structural and fluid damping is equal to zero, the system will become unstable. Since the instability is caused by the fluid stiffness, it is called fluid-stiffness-controlled instability.

The approach taken here is to present the integrated effect of the flow field on cylinder oscillations. The detailed flow field around the cylinders, its physical characteristics, and the origin of the flow variations have not been considered. Using this approach, as long as the system becomes unstable when $\zeta_f = 0$, we call it fluidelastic instability. In this sense, we ignore the physics of the flow field. When $\zeta_f = 0$, with either damping-controlled or stiffness-controlled instability, other effects, associated with vortex shedding and flow separation, may contribute to instability. These aspects of the problem have not been seriously studied in the past.

V. WHAT ARE THE VALUES OF THE EXPONENT OF THE MASS-DAMPING PARAMETER?

It is customary to combine the mass and damping together as a single parameter, called the mass-damping parameter. The stability criterion developed in the early 1970s (Connors 1970) shows that the critical flow velocity is proportional to the half power of the mass-damping parameter. Subsequently, other investigators (Weaver and Grover 1978, Chen and Jendrzejczyk 1981) found that the exponent may vary from 0 to 1. Other experimental data (Tanaka and Takahara 1981, Chen and Jendrzejcyzk 1983, Weaver and Fitzpatrick 1987) show that it may vary from 0 to ∞ depending on the array and range of δ_s ($= 2\pi\zeta m/\rho D^2$). In practice, the exponent is typically taken to be 0.5 although it is not necessarily correct to do so.

Experimental Data

Systematic studies of the exponent α have been performed for different tube arrays. This was accomplished by testing tube arrays with different damping values or mass ratios or a combination of both parameters. The exponents that are based on the experimental data are given in Table 2. The following features are noted:

- For a tube row, square arrays, and rotated square arrays, the exponent is 0.5 for large δ_s. The only exception is the value given by Price and Paidoussis (1987). Their value is based on a single elastic cylinder surrounded by rigid tubes. The reason for the deviation is not known.

- For normal and parallel triangular arrays, the exponent appears to be less than 0.5. In particular, for the normal triangular array, it is approximately 0.3.

- At low δ_s, no conclusion can be made regarding the exponent.

Table 2. Values of α in studies where critical flow velocity is a function of the mass-damping parameter

Investigators	Tube array	Mass-damping parameter	α
Connors (1970)	Tube row, T/D = 1.41	8 to 110	0.5
Ishigai et al. (1973)	Tube rows, T/D = 1.19, 1.34, 1.79, 2.14, 2.68	5 to 180	0.5
Tanaka (1980)	Tube row T/D = 1.33	20 to 130	0.5
Tanaka and Takahara (1981)	Square array P/D = T/D = 1.33	10 to 130	0.5
Chen (1984)	Tube rows and all tube arrays	> 4	0.5
Price and Paidoussis (1987)	Square array P/D = T/D = 1.5 (a single flexible cylinder only)	5 to 1000	0.25
Minakami and Ohtomi (1987)	Triangular array and rotated triangular array, P/D = 1.3	0.2 and 60	0.5
Weaver and Grover (1978)	Rotated triangular array, P/D = 1.375	2 to 30	0.21
Weaver and El-Kashlan (1980)	Rotated triangular array, P/D = 1.375	10 to 60	0.29

Design Guides

On the basis of available experimental data and mathematical models, several design guidelines are proposed. The exponents to the mass-damping parameter vary widely:

- Pettigrew et al. (1978): The exponent is 0.5 for all tube arrays and all δ_s.

- Chen (1984): The exponent depends on tube arrangements and δ_m. For large δ_s, it is 0.5, and for small δ_m, it varies from 0.05 to 0.2.

- Blevins (1984): For $0.25 < \delta_m$, $\alpha = 0.21$; for $0.25 \lesssim \delta_s \gtrsim 0.75$, $\alpha = 0$; and for $\delta_s > 0.75$, $\alpha = 0.5$.

- Weaver and Fitzpatrick (1987): The exponent depends on tube arrangement and δ_s. For large δ_s, it is 0.58 (45°, 90°), 0.40 (60°), and 0.3 (30°), and for small δ_s, it is zero.

Mathematical Models

The exponents based on different mathematical models are different.

- Quasi-Static Theory: Only fluid stiffness forces are considered. The critical flow velocity is proportional to the half power of the mass-damping parameter.

- Quasi-Steady Theory: In the quasi-steady theory, both fluid-damping and fluid stiffness forces are included. Fluid stiffness coefficients are independent of U_r; therefore, for fluid-stiffness-controlled instability, α is equal to 0.5. Fluid damping coefficients are a function of U_r. At low δ_m, no conclusion can be made regarding the value of α.

- Unsteady Flow Theory: At low δ_s, fluid force coefficients are a function of U_r; no conclusion can be made regarding the value of α. At large δ_s, all fluid force coefficients are approximately independent of U_r, and $\alpha = 0.5$.

From experimental data, mathematical models, and proposed design guidelines, some general conclusions can be made about the exponent.

- At high δ_s, mass ratio and damping ratio can be combined into a single parameter. However, at low δ_s, they generally cannot be combined into a single parameter.

- At high δ_s, since all fluid force coefficients are approximately independent of U_r, the exponent to the mass-damping parameter is 0.5.

- Although some of the data show that α is less than 0.5 for normal and parallel triangular arrays, if only these data at high δ_s are considered, the exponent is close to 0.5.

VI. WHAT MATHEMATICAL MODELS ARE APPROPRIATE?

Many mathematical models describe the instability of cylinder arrays in crossflow. These models can be classified according to three theories, as summarized in Table 3 (Chen 1987). Which one is appropriate?

This is a simple question, but it is difficult to provide a simple answer. Some general conclusions can be made.

- The unsteady flow theory includes all fluid effects; therefore, it is applicable in all parameter ranges. Unfortunately, at this time, it is not possible to base the prediction of the flow field on the unsteady flow theory.

- The quasi-steady flow theory is applicable to most cases, in particular, at high reduced flow velocity. It includes only fluid damping and fluid stiffness.

- The quasi-static flow theory is applicable to fluid-stiffness-controlled instability. Since fluid-damping forces are not included, no damping-controlled instability can be predicted. A single elastic cylinder in a rigid array will not become unstable.

For future development, the quasi-steady flow theory can be improved for large U_r and unsteady flow must be adopted for small U_r.

In the literature, different cylinder models are used to determine the critical flow velocity:

(1) Coupled-Mode Model: A group of flexible cylinders oscillating in an instability mode.

(2) Single-Cylinder Model: A single, flexible cylinder within a rigid array.

(3) Constrained-Mode Model: A group of flexible cylinders oscillating in a prescribed mode.

Table 3. Instability characteristics for different flow theories

Characteristic	Quasi-static flow theory	Quasi-steady flow theory	Unsteady flow theory
Fluid forces	Fluid stiffness Fluid stiffness	Fluid damping Fluid damping Fluid stiffness	Fluid inertia
Dependence of fluid force coefficients on U_r	No	Yes	Yes
Instability mechanism instability	Fluid-stiffness-controlled or fluid-damping-controlled instability	Fluid-stiffness-controlled controlled or fluid-damping-controlled instability	Fluid-stiffness-
Dominant terms in Eq. (10) in controlling instability	K_2 controlled instability	C_1 for fluid-damping-controlled instability K_2 for fluid-stiffness-	Same as quasi-steady flow theory
Minimum degrees of freedom to cause instability	Two	One	One
Multiple stability-instability regions	No	No	Yes
Effect of detuning	Important controlled instability, not important for fluid-damping-controlled instability	Important for stiffness-flow theory	Same as quasi-steady
Special form of instability criterion for constrained mode	$U_r = \delta^{0.5}$	$U_r = \delta^{0.5}$	$U_r = \alpha(U_r)\delta^{0.5}$

The critical flow velocity based on the coupled-mode model represents the true value and the mode represents the mode shape. The other two models are approximate solutions.

- Single-Cylinder Model: The coupling terms of various fluid force components are ignored. Only the fluid-damping-controlled type instability can be studied with the model; no fluid-stiffness-controlled type instability can be found when this model is used. The critical flow velocity determined from this model will be, in general, larger than that for a coupled-mode model.

- Constrained-Mode Model: In this model, the motion pattern is assumed, i.e., the instability may not actually be an instability mode. Therefore, the accuracy of the critical flow velocity depends on how good the assumed mode is. In most cases, the constrained-mode model will predict a higher critical flow velocity.

In a practical heat exchanger, there are often thousands of tubes. In such cases the coupled-mode model will involve thousands of equations. Do we need to include all tubes in the model? The answer is obviously no. In the practical case, the flow distributions are not uniform. Normally, only the critical areas must be examined. Of course, it requires some effort to identify the critical areas. Once these areas are specified, a finite group of cylinders can be included in the coupled-mode model. For different arrays, the following number of cylinders can be included to provide a reasonably accurate prediction:

- Tube Rows: Three flexible cylinders in a rigid row of cylinders,

- Square Array: Nine cylinders within a rigid array,

- Triangular Array: Seven cylinders within a rigid array.

Although neither complete analytical solutions nor experimental data for different tube arrays are available to compare the accuracy of the simplified coupled-mode model, it is expected that, for practical applications, a full coupled-mode model is not needed.

VII. CONCLUDING REMARKS

It is apparent that fluidelastic instabilities of a group of cylinders in crossflow is one of the most debated and confusing topics on the interactions between fluid and structure in recent history. It is fairly common that papers published on this subject contain incorrect statements. Furthermore, some of the incorrect statements are quoted by others working in this field.

Under such circumstances, designers and researchers are still facing some difficulty in resolving this problem. Designers can use available design guides. Design guides that are more reliable are needed to establish the critical flow velocity more precisely under different flow conditions. For researchers, this subject will remain a problem for further studies, including theoretical, numerical, and experimental programs.

In this report, a series of issues on this subject was discussed and appropriate solutions were pointed out. It is not possible to provide satisfactory answers to all questions. Nevertheless, these discussions will provide some guidelines on the future development of the subject and avoid unnecessary confusion and misunderstanding.

One of the issues, which has not been adequately addressed, is the physics of fluid across an array of cylinders. We can look at this problem from three viewpoints:

- Analytical Study: Practically no valid solutions are available for flow field around an array of oscillating cylinders. It is probably unlikely that an analytical prediction method can be developed for general arrays of cylinders in crossflow at the practical flow range, namely, moderate to high.

- Experimental Study: There are very limited studies on the flow field associated with cylinders oscillating in crossflow. Published data provide some insights into the physics of fluid, but many more tests are needed.

- Numerical Study: Numerical solutions for motion-dependent fluid forces for cylinders are not available. Although the numerical technique is expected to be useful in certain flow ranges, it is not expected to be applicable for the entire range of Reynolds number.

In the past, extensive efforts have been made to obtain the resultant effect, i.e., determination of the critical flow velocity. Very little attention has been paid to the physics. Until the physics of flow across cylinders is better understood, it will probably be difficult to make a significant contribution to the prediction of critical flow velocity.

ACKNOWLEDGMENTS

Figure 3 was provided by Joe Jendrzejczyk of Argonne National Laboratory.

This work was sponsored by the U.S. Department of Energy (DOE), Office of Energy Utilization Research, under the Energy Conversion and Utilization Technologies (ECUT) Program. The continuing encouragement and support of M. E. Gunn of US/DOE are appreciated.

REFERENCES

Axisa, F. et al. 1984. Vibration of Tube Bundles Subjected to Air-Water and Steam-Water Cross Flow: Preliminary Results on Fluidelastic Instability. In ASME Symp. on Flow-Induced Vibration, Vol. 2, New York, pp. 269-284.

Axisa, F. et al. 1986. Flow-Induced Vibration of Steam Generator Tubes. EPRI NP-4559, May 1986.

Blevins, R. D. 1984. Letter to the Editor. J. Sound Vib. 97, 641-644.

Chen, S. S. 1984. Guidelines for the Instability Flow Velocity of Tube Arrays in Crossflow. J. Sound Vib. 93, 439-455.

Chen, S. S. 1987. Flow-Induced Vibration of Circular Cylindrical Structures. Hemisphere Publishing Co., New York.

Chen, S. S. and Jendrzejczyk, J. A. 1981. Experiments on Fluid Elastic Instability in Tube Banks Subjected to Liquid Cross Flow. J. Sound Vib. 78, 355-381.

Chen, S. S. and Jendrzejczyk, J. A. 1983. Stability of Tube Arrays in Crossflow. Nucl. Eng. Des. 75, 351-374.

Chen, S. S. and Jendrzejczyk, J. A. 1986. Flow-Induced Vibration of the SSME LOX Posts. In Flow-Induced Vibration - 1986. ASME, New York, PVP-Vol. 104, pp. 119-126.

Chen, S. S. and Jendrzejczyk, J. A. 1987. Characteristics of Fluidelastic Instability of Tube Rows in Crossflow. Proc. Int. Conf. on Flow Induced Vibrations, Bowness-on-Windermere, England, May 12-14, 1987, Paper No. B3, pp. 77-84.

Connors, H. J. 1970. Fluidelastic Vibration of Tube Arrays Excited by Cross Flow. In Flow-Induced Vibration of Heat Exchangers, Reiff, D. D., Ed., ASME, New York, pp. 42-56.

Hara, F. 1987. Vibration of a Single Row of Circular Cylinders Subjected to Two-Phase Bubble Cross-Flow. Proc. Int. Conf. on Flow Induced Vibrations, Bowness-on-Windermere, England, May 12-14, 1987, Paper No. E1, pp. 203-210.

Ishigai, S., Nishikawa, Z., and Yagi, E. 1973. Structure of Gas Flow and Vibration in Tube Banks with Tube Axes Normal to Flow. In Int. Symp. on Marine Engineering, Tokyo, pp. 1-5-23 to 1-5-33.

Minakami, K. and Ohtomi, K. 1987. Flow Direction and Fluid Density Effects on the Fluidelastic Vibrations of a Triangular Array of Tubes. Proc. Int. Conf. on Flow Induced Vibrations, Bowness-on-Windermere, England, May 12-14, 1987, Paper No. B2, pp. 65-75.

Paidoussis, M. P. 1987. Flow-Induced Instabilities of Cylindrical Structures. Appl. Mech. Rev. 40, 163-175.

Pettigrew, M. J., Sylvestre, Y., and Campagna, A. O. 1978. Vibration Analysis of Heat Exchanger and Steam Generator Designs. Nucl. Eng. Des. 48, 97-115.

Price, S. J., and Paidoussis, M. P. 1987. The Flow-Induced Response of a Single Flexible Cylinder in an In-Line Array of Rigid Cylinders. Proc. Int. Conf. on Flow Induced Vibrations, Bowness-on-Windermere, England, May 12-14, 1987, Paper No. B1, pp. 51-63.

Soper, B. M. H. 1980. The Effect of Tube Layout on the Fluidelastic Instability of Tube Bundles in Cross Flow. In Flow-Induced Heat Exchanger Tube Vibration - 1980, Chenoweth, J. M., and Stenner, J. R., Eds., ASME, New York, pp. 1-9.

Tanaka, H. 1980. Study on Fluidelastic Vibrations of Tube Bundle. J. Soc. Mech. Eng., Trans., Section B 46, 1397-1407.

Tanaka, H. and Takahara, S. 1981. Fluid Elastic Vibration of Tube Array in Cross Flow. J. Sound Vib. 77, 19-37.

Weaver, D. S. and El-Kashlan, M. 1981. The Effect of Damping and Mass Ratio on the Stability of a Tube Bank. J. Sound Vib. 76, 283-294.

Weaver, D. S. and Fitzpatrick, J. A. 1987. A Review of Flow Induced Vibrations in Heat Exchangers. Proc. Int. Conf. on Flow Induced Vibrations, Bowness-on-Windermere, England, May 12-14, 1987, Paper No. A1, pp. 1-17.

Weaver, D. S. and Grover, L. K. 1978. Cross-Flow Induced Vibrations in a Tube Bank - Turbulent Buffeting and Fluid Elastic Instability. J. Sound Vib. 59, 177-194.

Yeung, H. and Weaver, D. S. 1983. The Effect of Approach Flow Direction on the Flow Induced Vibrations of a Triangular Tube Array. J. Mech. Des. 105, 76-82.

APPENDIX: AN UNSTEADY FLOW MODEL FOR FLUIDELASTIC INSTABILITY OF A GROUP OF CIRCULAR CYLINDERS IN CROSSFLOW

1. Equations of Motion

Consider a group of N identical circular cylinders with radius R (= D/2) subjected to crossflow as shown in Fig. A.1. The axes of the cylinders are parallel to the z axis and flow is parallel to the x axis. The subscript j is used to denote variables associated with cylinder j. The variables associated with the cylinder motion in the x and y directions are flexural rigidty EI, cylinder mass per unit length m, structural damping coefficient C_s, and displacement u_j and v_j. The equations of motion for cylinder j in the x and y directions are (Chen and Jendrzejczyk 1983)

$$EI \frac{\partial^4 u_j}{\partial z^4} + C_s \frac{\partial u_j}{\partial t} + m \frac{\partial^2 u_j}{\partial t^2} + \sum_{k=1}^{N} \rho\pi R^2 \left(\alpha_{jk} \frac{\partial^2 u_k}{\partial t^2} + \sigma_{jk} \frac{\partial^2 v_k}{\partial t^2}\right)$$

$$+ \sum_{k=1}^{N} \left[\left(\bar{\alpha}'_{ojk} + \frac{\rho U^2}{\omega} \alpha'_{jk}\right) \frac{\partial u_k}{\partial t} + \left(\bar{\sigma}'_{ojk} + \frac{\rho U^2}{\omega} \sigma'_{jk}\right) \frac{\partial v_k}{\partial t}\right]$$

$$+ \sum_{k=1}^{N} \rho U^2 (\alpha''_{jk} u_k + \sigma''_{jk} v_k) = 0 , \qquad \text{(A.1)}$$

$$EI \frac{\partial^4 v_j}{\partial z^4} + C_s \frac{\partial v_j}{\partial t} + m \frac{\partial^2 v_j}{\partial t^2} + \sum_{k=1}^{N} \rho\pi R^2 \left(\tau_{jk} \frac{\partial^2 u_k}{\partial t^2} + \beta_{jk} \frac{\partial^2 v_k}{\partial t^2}\right)$$

$$+ \sum_{k=1}^{N} \left[\left(\bar{\tau}'_{ojk} + \frac{\rho U^2}{\omega} \tau'_{jk}\right) \frac{\partial u_k}{\partial t} + \left(\bar{\beta}'_{ojk} + \frac{\rho U^2}{\omega} \beta'_{jk}\right) \frac{\partial v_k}{\partial t}\right]$$

$$+ \sum_{k=1}^{N} \rho U^2 (\tau''_{jk} u_k + \beta''_{jk}) = 0 , \qquad \text{(A.2)}$$

where t is time; ρ is fluid density; U is flow velocity; ω is circular frequency of oscillations; α_{jk}, σ_{jk}, τ_{jk}, and β_{jk} are added-mass coefficients; $\bar{\alpha}'_{ojk}$, $\bar{\sigma}'_{ojk}$, $\bar{\tau}'_{ojk}$, and $\bar{\beta}'_{ojk}$ are fluid viscous damping at zero flow velocity; α'_{jk}, σ'_{jk}, τ'_{jk}, and β'_{jk} are fluid damping coefficients attributed to flow; and α''_{jk}, σ''_{jk}, τ''_{jk}, and β''_{jk} are fluid stiffness coefficients. Note that fluid damping coefficients and fluid stiffness coefficients are functions of reduced flow velocity U_r (= $U/f_f D$; f_f is the oscillation frequency of the cylinders).

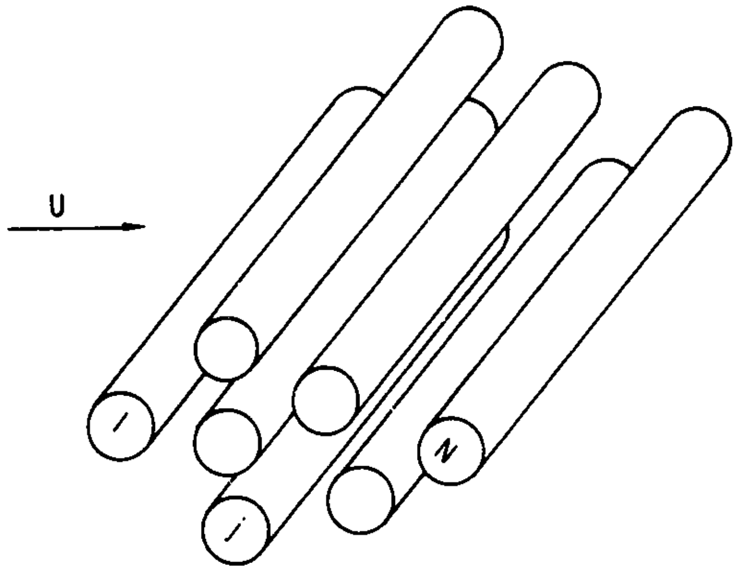

(a) A GROUP OF CIRCULAR CYLINDERS

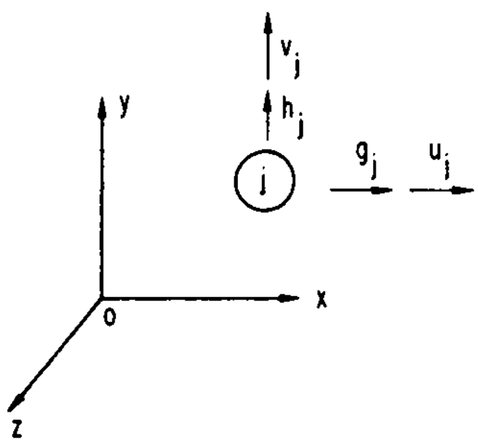

(b) FLUID FORCE AND CYLINDER DISPLACEMENT COMPONENTS

Fig. A.1. A group of cylinders in crossflow

The in-vacuum variables are mass per unit length m, modal damping ratio ζ_v, and natural frequency f_v ($= \omega_v/2\pi$). The values for f_v and ζ_v can be calculated from the equation of motion and appropriate boundary conditons, or from tests in vacuum (practically in air). The modal function of the cylinder vibrating in vacuum and in fluid is $\psi(z)$;

$$\frac{1}{\ell}\int_o^{\ell} \psi^2(z)dz = 1 \ , \tag{A.3}$$

where ℓ is the length of the cylinders. Let

$$u_j(z,t) = a_j(t)\psi(z) \ ,$$
$$v_j(z,t) = b_j(t)\psi(z) \ , \tag{A.4}$$

where $a_j(t)$ and $b_j(t)$ are functions of time only. Calculation of Eqs. (A.1) and (A.2) yields

$$\frac{d^2a_j}{dt^2} + 2\zeta_v\omega_v \frac{da_j}{dt} + \omega_v^2 a_j + \frac{\rho\pi R^2}{m}\sum_{k=1}^{N}\left(\alpha_{jk}\frac{d^2a_k}{dt^2} + \sigma_{jk}\frac{d^2b_k}{dt^2}\right)$$
$$+ \sum_{k=1}^{N}\left(\frac{\bar{\alpha}'_{ojk}}{m}\frac{da_k}{dt} + \frac{\bar{\sigma}'_{ojk}}{m}\frac{db_k}{dt}\right) - \frac{\rho U^2}{m\omega}\sum_{k=1}^{N}\left(\alpha'_{jk}\frac{da_k}{dt} + \sigma'_{jk}\frac{db_k}{dt}\right)$$
$$- \frac{\rho U^2}{m}\sum_{k=1}^{N}\left(\alpha''_{jk}a_k + \sigma''_{jk}b_k\right) = 0 \ ,$$

(A.5)

$$\frac{d^2b_j}{dt^2} + 2\zeta_v\omega_v \frac{db_j}{dt} + \omega_v^2 b_j + \frac{\rho\pi R^2}{m}\sum_{k=1}^{N}\left(\tau_{jk}\frac{d^2a_k}{dt^2} + \beta_{jk}\frac{d^2b_k}{dt^2}\right)$$
$$+ \sum_{k=1}^{N}\left(\frac{\bar{\tau}'_{ojk}}{m}\frac{da_k}{\partial t} + \frac{\bar{\beta}_{ojk}}{m}\frac{db_k}{\partial t}\right) - \frac{\rho U^2}{m\omega}\sum_{k=1}^{N}\left(\tau'_{jk}\frac{d^2a_k}{dt} + \beta'_{jk}\frac{db_k}{dt}\right)$$
$$- \frac{\rho U^2}{m}\sum_{k=1}^{N}\left(\tau''_{jk}a_k + \beta''_{jk}b_k\right) = 0 \ .$$

When the dimensionless parameters are

$$\frac{\bar{\alpha}'_{ojk}}{m\omega_v} = \alpha'_{ojk} \,, \qquad U_v = \frac{U}{f_v D} \,,$$

$$\frac{\bar{\sigma}'_{ojk}}{m\omega_v} = \sigma'_{ojk} \,, \qquad \gamma = \frac{\rho \pi R^2}{m} \,,$$

$$\frac{\bar{\tau}'_{ojk}}{m\omega_v} = \tau'_{ojk} \,, \tag{A.6}$$

$$\frac{\bar{\beta}'_{ojk}}{m\omega_v} = \beta'_{ojk} \,,$$

Eqs. (A.5) become

$$\ddot{a}_j + \gamma \sum_{k=1}^{N} (\alpha_{jk}\ddot{a}_k + \sigma_{jk}\ddot{b}_k) + 2\zeta_v \omega_v \dot{a}_j + \sum_{k=1}^{N} \omega_v(\alpha'_{ojk}\dot{a}_k + \sigma'_{ojk}\dot{b}_k)$$

$$- \frac{\gamma}{\pi^3} U_v^2 \left(\frac{\omega_v^2}{\omega}\right) \sum_{k=1}^{N} (\alpha'_{jk}\dot{a}_k + \sigma'_{jk}\dot{b}_k)$$

$$+ \omega_v a_j - \frac{\gamma}{\pi^3} U_v^2 \omega_v^2 \sum_{k=1}^{N} (\alpha''_{jk}a_k + \sigma''_{jk}b_k) = 0 \,, \tag{A.7}$$

$$\ddot{b}_j + \gamma \sum_{k=1}^{N} (\tau_{jk}\ddot{a}_k + \beta_{jk}\ddot{b}_k) + 2\zeta_v \omega_v \dot{b}_j + \sum_{k=1}^{N} \omega_v(\tau'_{ojk}\dot{a}_k + \beta'_{ojk}\dot{b}_k)$$

$$- \frac{\gamma}{\pi^3} U_v^2 \left(\frac{\omega_v^2}{\omega}\right) \sum_{k=1}^{N} (\tau'_{jk}\dot{a}_k + \beta'_{jk}\dot{b}_k)$$

$$+ \omega_v^2 b_j - \frac{\gamma}{\pi^3} U_v^2 \omega_v^2 \sum_{k=1}^{N} (\tau''_{jk}a_k + \beta''_{jk}b_k) = 0 \,, \tag{A.8}$$

where the dot denotes differentiation with respect to t.

2. Vibration in Quiescent Fluid

In quiescent fluid, $U_v = 0$,

$$\ddot{a}_j + \gamma \sum_{k=1}^{N} (\alpha_{jk}\ddot{a}_j + \sigma_{jk}\ddot{b}_k)$$

$$+ 2\zeta_v\omega_v\dot{a}_j + \sum_{k=1}^{N} \omega_v(\alpha'_{ojk}\dot{a}_k + \sigma'_{ojk}\dot{b}_k)$$

$$+ \omega_v^2 a_j = 0 \ , \qquad \text{(A.9)}$$

$$\ddot{b}_j + \gamma \sum_{k=1}^{N} (\tau_{jk}\ddot{a}_k + \beta_{jk}\ddot{b}_k)$$

$$+ 2\zeta_v\omega_v\dot{b}_j + \sum_{k=1}^{N} \omega_v(\tau'_{ojk}\dot{a}_k + \beta'_{ojk}\dot{b}_k)$$

$$+ \omega_v^2 b_j = 0 \ . \qquad \text{(A.10)}$$

From Eqs. (A.9) and (A.10), the vibrational characteristics in quiescent fluid can be calculated. These include uncoupled and coupled vibration.

Uncoupled Vibration: A flexible cylinder vibrates in an array of rigid cylinders. All coupling terms can be ignored. For example

$$(1 + \gamma\alpha_{jj})\ddot{a}_j + (2\zeta_v + \alpha'_{ojj})\omega_v\dot{a}_j + \omega_v a_j = 0 \ . \qquad \text{(A.11)}$$

From Eq. (A.11), it is easily shown that, for uncoupled vibration, the effective mass m_u, natural frequency ω_u, and damping ζ_u are given by

$$m_u = m + \rho\pi R^2\alpha_{jj} \ ,$$

$$\omega_u = \frac{\omega_v}{(1 + \gamma\alpha_{jj})^{0.5}} \ , \qquad \text{(A.12)}$$

$$\zeta_u = \frac{\zeta_v + 0.5\alpha'_{ojj}}{(1 + \gamma\alpha_{jj})^{0.5}} \ .$$

There are N natural frequencies and damping values for a group of N cylinders. In Eqs. (A.12), if α_{jj} and α'_{ojj} are replaced by β_{jj} and β'_{ojj} respectively, the results correspond to the motion in the y direction.

Coupled Vibration: When all cylinders are flexible, the motions are coupled. The effective mass, modal damping, and natural frequency can be calculated from Eqs. (A.9) and (A.10). These parameters are denoted by m_c, f_c, and ζ_c.

Very simple results can be obtained with Eqs. (A.9) and (A.10) and the symmetric property of the added-mass coefficients for α_{jk}, σ_{jk}, τ_{jk}, and β_{jk}. Let the added-mass matrix be

$$[\gamma_{pq}] = \begin{bmatrix} \alpha_{jk} & \sigma_{jk} \\ \tau_{jk} & \beta_{jk} \end{bmatrix} , \quad j,k = 1 \text{ to } N , \quad p,q = 1 \text{ to } 2N . \tag{A.13}$$

Since γ_{pq} is symmetric, there are 2N eigenvalues which are positive numbers and denoted by μ_p (p = 1 to 2N), and the corresponding normalized eigenvectors are given by $\{e_p\}$; i.e.,

$$[\gamma_{pq}]\{e_q\} = \mu_p\{e_p\} . \tag{A.14}$$

Let E be the modal matrix formed from the column of eigenvectors, and the damping matrix d_{pq} be

$$[D] = [d_{pq}] = \begin{bmatrix} \alpha'_{ojk} & \sigma'_{ojk} \\ \tau'_{ojk} & \beta'_{ojk} \end{bmatrix} , \quad j,k = 1 \text{ to } N , \quad p,q = 1 \text{ to } 2N , \tag{A.15}$$

and

$$[\zeta_{pq}] = [E]^T[D][E] , \quad p,q = 1 \text{ to } 2N . \tag{A.16}$$

The values of m_c, f_c, and ζ_c are then given by

$$\begin{aligned} m_c &= m + \rho\pi R^2\mu_p , \\ \omega_c &= \frac{\omega_v}{(1 + \gamma\mu_p)^{0.5}} , \\ \zeta_c &= \frac{1}{(1 + \gamma\mu_p)^{0.5}} (\zeta_v + 0.5\,\zeta_{pp}) . \end{aligned} \tag{A.17}$$

There are 2N natural frequencies and modal damping values corresponding to the 2N coupled modes. In Eq. (A.17), the coupling terms due to fluid damping γ_{pq} ($p \neq q$) have been ignored; the results are the approximate solution for modal damping of coupled modes. Alternatively, the exact solutions of natural frequency f_c and modal damping ratio ζ_c can be calculated directly from Eqs. (A.9) and (A.10).

3. Vibration in Flowing Fluid

In flowing fluid, Eqs. (A.7) and (A.8) describe the motion of an array of cylinders. From these two equations, the natural frequencies and modal damping ratios of the system can be calculated as follows:

$$f_f = f_f(\gamma,\zeta_v,U_v) \ ,$$

$$\zeta_f = \zeta_f(\gamma,\zeta_v,U_v) \ . \tag{A.18}$$

The stability of a cylinder array is determined from Eqs. (A.7) and (A.8). The nondimensional parameters in Eqs. (A.7) and (A.8) are γ, ζ_v, U_v, α_{jk}, σ_{jk}, τ_{jk}, β_{jk}, α'_{ojk}, σ'_{ojk}, τ'_{ojk}, β'_{ojk}, α'_{jk}, σ'_{jk}, τ'_{jk}, β'_{jk}, α''_{jk}, σ''_{jk}, τ''_{jk}, and β''_{jk}. Therefore, the critical flow velocity can be written in a functional form as

$$U_v = F(\gamma,\zeta_v,\omega_v/\omega,\alpha_{jk},\sigma_{jk},\tau_{jk},\beta_{jk},\alpha'_{ojk},\sigma'_{ojk},\tau'_{ojk},\beta'_{ojk},$$

$$\alpha'_{jk},\sigma'_{jk},\tau'_{jk},\beta'_{jk},\alpha''_{jk},\sigma''_{jk},\tau''_{jk},\beta''_{jk}) \ . \tag{A.19}$$

For a given array of cylinders, if fluid force coefficients are independent of U_v, then

$$U_r = F(\gamma,\zeta_v) \ , \tag{A.20}$$

i.e., the critical flow velocity is a function of mass ratio and damping ratio only.

In light fluid, fluid inertia and damping associated with the quiescent fluid can be neglected. Equations (A.7) and (A.8) can be written

$$\ddot{a}_j + 2\zeta_v\omega_v\dot{a}_j + \omega_v^2 a_j$$

$$- \frac{\gamma}{\pi^3} U_v^2 \sum_{k=1}^{N} \left[\frac{\omega_v^2}{\omega} (\alpha'_{jk}\dot{a}_k + \sigma'_{jk}\dot{b}_k) + \omega_v^2(\alpha''_{jk}a_k + \sigma''_{jk}b_k)\right] = 0 \ , \tag{A.21}$$

$$\ddot{b}_j + 2\zeta_v \omega_v \dot{b}_j + \omega_v^2 b_j - \frac{\gamma}{\pi^3} U_v^2 \sum_{k=1}^{N} \left[\frac{\omega_v^2}{\omega} (\tau'_{jk}\dot{a}_k + \beta'_{jk}\dot{b}_k) + \omega_v^2(\tau''_{jk}a_k + \beta''_{jk}b_k)\right] = 0 \ . \qquad \text{(A.21) (Contd.)}$$

In light fluid, all fluid force coefficients are approximately independent of U_v and the oscillation frequency is approximately equal to ω_v. Then γU_v^2 plays the same role as ζ_v; both of them contribute to system damping. The modal damping for a particular mode can be written

$$\zeta_f = \zeta_v - C \gamma U_v^2 \ , \qquad \text{(A.22)}$$

where C depends on fluid damping and fluid stiffness coefficients. Instability occurs if $\zeta_f = 0$; i.e.,

$$U_v = \frac{1}{C} \left(\frac{\zeta_v}{\gamma}\right)^{0.5}$$

or (A.23)

$$\frac{U}{f_v D} \alpha \left(\frac{2\pi\zeta_v m}{\rho D^2}\right)^{0.5} \ .$$

Thus, the critical flow velocity is a function of the mass-damping parameter and proportional to its half power.

Distribution for ANL-87-47

Internal:

S. S. Chen (15)
H. H. Chung
H. Drucker
H. Halle
R. E. Holtz
J. A. Jendrzejczyk
C. A. Kot
T. M. Mulcahy
C. Panchal
T. J. Rabas
W. W. Schertz
E. M. Stefanski
A. Thomas
C. E. Till
M. W. Wambsganss
R. W. Weeks
ANL Patent Dept.
ANL Contract File
ANL Libraries
TIS Files (3)

External:

DOE-TIC for distribution per UC-95f (169)
Manager, Chicago Operations Office, DOE
Director, Technology Management Div., DOE-CH
D. L. Bray, DOE-CH
A. L. Taboas, DOE-CH
P. Alexander, Combustion Engineering, Rochester, NY
S. J. Green, EPRI
R. A. Greenkorn, Purdue University
L. J. Jardine, Bechtel, San Francisco, CA
C. Y. Li, Cornell University
P. G. Shewmon, Ohio State University
R. E. Smith, EPRI
G. L. Anderson, ARO
H. L. Anderson, Ontario Hydro
M. K. Au-Yang, B&W
K. J. Bell, Oklahoma State University
A. E. Bergles, RPI
M. D. Bernstein, FWEC
R. D. Blevins, Rohr Industries
J. C. Blomgren, Commonwealth Edison
G. N. Bogel, Dow Chemical U.S.A.
G. J. Bohm, Westinghouse PWR Systems
G. Borushko, Westfield, NJ
H. W. Braun, IMO Delaval
G. M. Cameron, Chemetics International
C. C. Chamis, NASA/Lewis
C. A. Chandley, TVA
S. Chandra, Northeast Utilities
P. Y. Chen, NRC
J. M. Chenoweth, HTRI
M. A. Chionchio, Southwestern Engineering
D. Chisholm, HTRI
C. Chiu, Southern California Edison Co.
H. J. Connors, Westinghouse R&D
R. J. Croke, Stone & Webster Engineering Corp.
J. L. Dixon, Southern Heat Exchanger Corp.
J. J. Eberhardt, DOE/Conservation

F. L. Eisinger, FWEC
R. L. Eshleman, Vibration Institute
D. F. Fijas, ITT Standard
R. J. Fritz, GE/KAPL
N. R. Gainsboro, Southwestern Engineering
C. C. Gentry, Phillips Petroleum Company
O. Goetz, NASA/MSFC
J. S. Gosnell, Braidwood Nuclear Power Station
O. M. Griffin, Naval Research Lab.
K. G. Grinnell, Graham Mfg. Co.
M. E. Gunn, DOE/Conservation (2)
R. J. Hansen, Naval Research Lab.
R. T. Hartlen, Ontario Hydro
K. H. Haslinger, CE
G. Hausenbauer, Struther-Wells
T. G. Haynes, Duke Power
T. D. Hazell, Foster Wheeler
W. J. Heilker, CE
L. W. Heilmann, Nooter Corp.
T. G. Heilmann, Chemetics International
B. Johnson, Pacific Northwest
D. L. Johnson, M. W. Kellogg Company
A. E. Jones, E. I. du Pont
A. V. Karvelis, Borg-Warner
E. Kiss, General Electric Co.
J. H. Kissel, ITT Standard
P. A. Larsen, Amoco Oil Co.
M. LeFevre, Research Cottrell
S. F. Lindsey, Duke Power
B. T. Lubin, CE
P. J. Marto, U.S. Naval Postgraduate School
A. J. Meehan, Word Industries
J. Mills, INEL
P. M. Moretti, Oklahoma State Univ.
A. Morris, TVA
T. J. Muldoon, Heat Transfer Specialists
K. Nelson, Manning & Lewis Eng.
E. H. Novendstern, Westinghouse Electric Corp.
T. M. O'Connor, M. W. Kellogg Co.
S. Oppegaard, Commonwealth Edison
R. Penney, A. E. Staley Company
S. M. Peters, HTRI
L. Povinelli, NASA/Lewis
S. Proctor, Monsanto Company
J. Rajan, NRC
M. M. Reischmann, Office of Naval Research
J. F. Reiss, Commonwealth Edison
S. Richlen, DOE/OIP
R. B. Ritter, Fluor Engrs & Constructors
D. Rockwell, Lehigh University
T. M. Rudy, Exxon R&D Labs
J. B. Sandifer, B&W/ARC
S. D. Savkar, GE/CRD
M. Sax, Westinghouse Bettis
J. E. Schroeder, Nooter Corporation
R. K. Shah, Harrison Radiator
Y. S. Shin, U.S. Naval Postgraduate School
W. Simmons, General Dynamics
L. L. Simpson, Union Carbide
K. P. Singh, Holtec International
N. R. Singleton, Westinghouse Electric Corp.
N. Sondergaard, David Taylor Naval Ship Research & Development Center
D. Steininger, EPRI
H. Struck, NASA/MSFC
A. L. Sudduth, Duke Power Co.
K. K. Tam, Amoco Oil Co.
W. H. Thielbahr, DOE/ID
M. R. Torres, General Electric Co.
S. N. Tower, Westinghouse Monroeville
J. Tsou, EPRI
M. E. Underwood, Badger Co.
G. H. Weidenhamer, NRC/RES
J. Yampolsky, GA Technologies, Inc.
E. A. Zanoni, Westinghouse Bettis